Multicomponent Crystals of an Artemisinin Derivative and Cinchona Alkaloids for Use as Antimalarial Drugs

Qi Jiang*, David A. Hirsh, Yifan Tu and Laibin Luo

Material and Analytical Sciences, Boehringer Ingelheim Pharmaceuticals, Inc. 900 Ridgebury Road/P.O. Box 368, Ridgefield, CT 06877 (USA). E-mail: qi.jiang@boehringer-ingelheim.com

Electronic Supplementary Information (ESI)

Contents

Figure S7. Crystal unit cell packing from Quinine hydrochloride dihydrate (QN HCl·2H_2O) single crystal structures. The stoichiometry of QN:HCl:H_2O is 1:1:2 according to the triclinic space group *P*1 with *Z*=2. From the single crystal structure, it is clearly to see the aliphatic amine group in QN molecule is protonated.

Table S6. Crystal Structure data and structural refinement information for QN HCl·2H_2O single crystal

Figure S8. ^{13}C MAS (ν_{rot} = 12 kHz) SSNMR spectra used for peak assignments of AS.

Figure S9. ^{13}C MAS (ν_{rot} = 12 kHz) SSNMR spectra used for peak assignments of CND.

Figure S10. ^{13}C MAS (ν_{rot} = 12 kHz) SSNMR spectra used for peak assignments of AS-CND.

Figure S11. ^{13}C MAS (ν_{rot} = 12 kHz) SSNMR spectra used for peak assignments of QN.

Figure S12. ^{13}C MAS (ν_{rot} = 12 kHz) SSNMR spectra used for peak assignments of QN HCl·2H_2O.

Figure S13. ^{1}H Solution NMR spectra of the starting materials and MCCs: a) QN; b) CND; c) AS; d) AS-CND; e) AS-QN.

Table S7. ^{1}H experimental solution NMR parameters

Table S8. ^{1}H-^{15}N CP/MAS (ν_{rot} = 12 kHz) experimental SSNMR parameters

Figure S14. ^{1}H-^{15}N CP/MAS (ν_{rot} = 12 kHz) SSNMR spectra showing expanded regions around the peaks.

Table S9. Experimental and calculated isotropic ^{15}N chemical shifts for the nitrogen-containing compounds in this work.

Figure S15. Experimental solubility results for both MCCs and all starting materials (AS, QN and CND) in PBS buffer solution at room temperature with three different pH values: 2.0, 6.8 and 7.4. for 2h and 24 h. A) Solubility of AS and B) Solubility of QN and CND.

Figure S16. PXRD patterns MCCs after solubility test (PBS buffer solution at 25 C) in different conditions. All PXRD patterns are compared with the starting materials and corresponding single components. A) AS-QN and B) AS-CND.

Table S10. Solubility data of both salts and starting materials in aqueous solution with three different pH values for 2 hr and 24 hr equilibrium time.

Reference

Experimental Section

Artesunate (AS), Artemisinin (ART), Dihydroartemisinin (DHA) and Artemether (AM) were purchased from Fisher Scientific. All cinchona alkaloids, including Quinine (QN), Quinidine (QND), Cinchonine (CN), Cinchonidine (CND) and Quinine hydrochloride dihydrate (QN HCl·2H_2O) were purchased from SigmaAldrich. All chemicals were used without purification.

Liquid Assistant Grinding (LAG). LAG is performed in small scale ball milling instrument with 5 mL milling jar with PTFE inlet and zirconia ball. Measure stoichiometrically amount two counterparts with 1:1 ratio and add small amount of MeOH for grinding with η=0.2 [η=Volume of solvent (μL)/Amount of solid (mg)].[1] The ball milling time is 30 minute at 30 Hz frequency. Characterization with powder X-ray diffraction (PXRD) after ball milling with comparison of starting materials.

Crystallization and Single Crystal Growth of Multicomponent Crystals (MCCs). Measure stoichiometrically 1:1 ratio of AS and QN or CND and dissolve in isopropanol at room temperature, and crystallization start in 2 hr with completion after antisolvent addition of n-heptane. After crystallization, samples are filtrated and dry at room temperature. The other cinchona alkaloids, QND and CN are tried at same conditions, no crystallization is performed. Single crystal is growth through slow solvent diffusion in small glass vial with isopropanol/n-heptane solvent system.

Powder X-ray Diffraction (PXRD). PXRD patterns are collected on Bruker D8 ADVANCE DAVINCI diffractometer equipped with LYNXEYE detector. The X-ray is generated by seal Cu tube for CuKα (λ = 1.54178 Å) at 40 kV and 40 mA. PXRD collection is performed through 2θ range between 2° to 35° with step of 0.015°/sec and data is analysed by DIFFRAC EVA.[2]

Thermal Analysis. Differential Scanning Calorimetry (DSC) is characterized by TA instrument DSC Q2000 and Thermogravimetric Analysis (TGA) is characterized by TA instrument TGA Q500. The temperature heating ramp is 10 °C/min from 30 °C to 250 °C.

Dynamic Vapor Sorption (DVS). DVS data is collected on SMS Advantage 1 instrument with 0 to 90 % RH at 25 C. The equilibrium condition at each humidity point is around dm/dt = 0.002.

Polarized Light Microscopy (PLM). PLM images are collected by Zeiss Axioskop 40 polarized light microscope. Samples are dispersed in Cargille Type A oil then examined in plane and cross polarized light.

Optical Rotation. The optical rotation of AS-QN and AS-CND salts are characterized in Rudolph Research Analytical Autopol III Automatic Polarimeter with wavelength 589 nm (Sodium D-line), and the concentration is c=1.0 in MeOH at 22 °C.

Single Crystal X-ray Diffraction (SCXRD). Single crystal data is collected on a Bruker X8 Prospector diffractometer equipped with a CuKα IμS microsource (λ = 1.54178 Å) and a PHOTON II CMOS detector at 100 K controlled with an Oxford cryosystem. Data integration of intensities and refinement of cell parameter is accomplished using APEX3 software.[3] The structure is solved using OLEX2 software package with structure solution program SHELXT and refined with the SHELXL refinement package using least squares minimisation.[4] All non-hydrogen atoms are refined with anisotropic atomic displacement parameters. Hydrogen atoms are located from the difference Fourier electron density map. All hydrogen atoms are refined using isotropic atomic displacement parameters.

Solid-State NMR (SSNMR). All SSNMR experiments were conducted using a Bruker Avance III NMR spectrometer, a Bruker B_0 = 9.4 T magnet (^{1}H = 400.46 MHz, ^{13}C = 100.69 MHz, ^{15}N = 40.58 MHz), and a 4 mm Bruker BL4 DVT probe. All spectra were referenced to TMS at 0 ppm following the unified scale in the IUPAC standard.[5] This referencing corresponds to the high frequency ^{13}C peak of adamantane at 38.48 ppm, and ^{15}N signal of $^{15}NH_4Cl$ at 39.3 ppm.[6] ^{13}C and ^{15}N spectra were measured

using a standard 1H-X cross polarization (CP) sequence with a ramped-amplitude spin-lock pulse[7-9] on the ^{1}H channel, and SPINAL-64 decoupling.[10] Spinning sidebands were removed from the ^{13}C spectra using TOtal Supression of Sidebands (TOSS).[11] Additional ^{13}C experiments for signal assignment were conducted using the CPPI[12] and FSLG-HETCOR[13] sequences. Full SSNMR parameters are given in Table S3, S4 and S8.

Solution NMR. ^{1}H solution NMR spectra were acquired on a Bruker Avance III NMR spectrometer, a Bruker B_0 = 11.7 T magnet (^{1}H = 500.13 MHz) and a triple-channel 5 mm PABBO BB probe. Samples were dissolved in DMSO-d_6. Referencing was performed using the residual ^{1}H signal of the solvent, at 2.5 ppm. The solution NMR parameters are given in Table S6

CASTEP DFT Calculations. Density functional theory calculations of ^{13}C and ^{15}N chemical shieldings were conducted using the CASTEP module of Biovia Materials Studio 2020.[14-16] Calculations used the Perdew–Burke–Ernzerhof (PBE) functional,[17] and included dispersion corrections according to Tkatchenko and Scheffler (TS).[18] Calculated chemical shieldings (σ_{calc}) were converted into chemical shifts (δ_{iso}) using the relationship: $\delta_{iso}=\sigma_{ref}-\sigma_{calc}$, where σ_{ref} was determined by comparing the mean of the experimental isotropic chemical shifts and calculated shieldings ($\sigma_{ref,\ 13C}$ = 170 ppm, $\sigma_{ref,\ 15N}$ = 222.2 ppm).

Solubility Test. Around 20 mg of powder were weighed and transferred into 8 mL glass vials. 2 mL of PBS buffer (pH adjusted to 2.0, 6.8 and 7.4) was added into vials. Then, vials were set on rotators and rotated at the rate of 30 rpm. 400µl of suspension from each vial was collected at 2 hr and 24 hr time point. The samples were then loaded into insert filtration 0.2 µm membrane and centrifuged at 200 rpm for 10 min. 100µl of the filtrated samples was collected for sample analysis. Samples were diluted 200X (for AS) or 20000X (for QN and CND) by diluent (acetonitrile:water=1:1). Samples were further analyzed by LC-MS after dilution. The chromatograph separation was conducted on Waters Acquity system and Acquity UPLC BEH C-18 column (1.7µM, 1.0*50mm). The mobile phases were 0.1% formic acid in water and acetonitrile. The MS analysis was conducted on ABSiex Qtrap 6500. The analysis was conducted on positive mode.

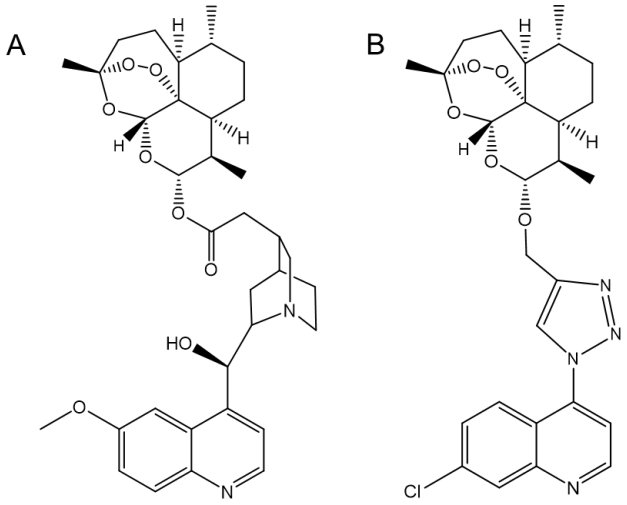

Figure S1. Synthetic molecular structures of artemisinin and quinoline hybrids. A) First example of an artemisinin-quinine hybrid.[19] B) Artemisinin-chloroquine hybrid synthesized by click chemistry.[20]

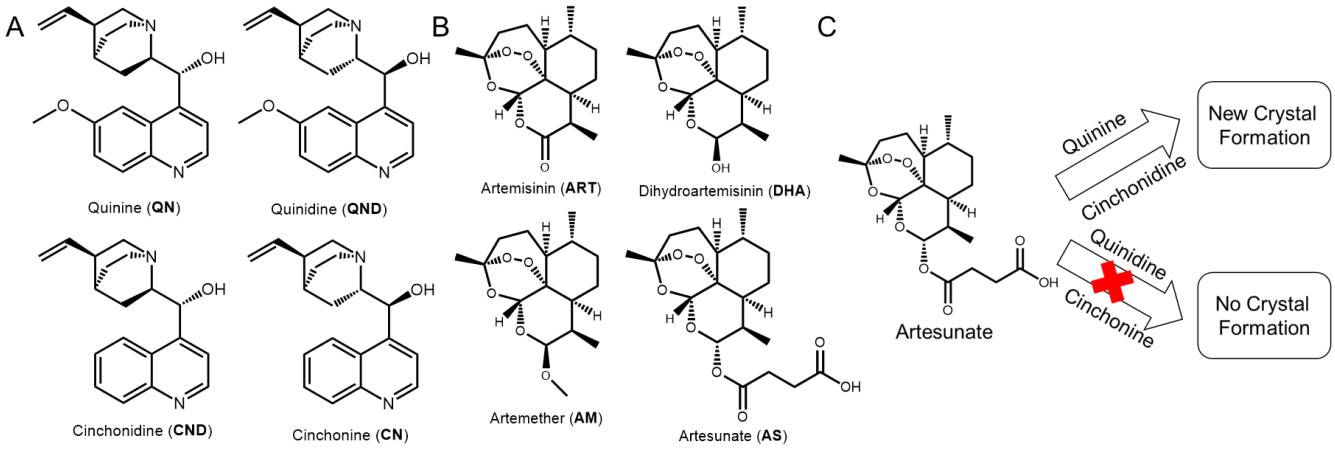

Figure S2. A) Chemical structures of cinchona alkaloids with quinolines: Quinine (QN), Quinidine (QND), Cinchonidine (CND), and Cinchonine (CN). B) Chemical structures of Artemisinin (ART) and semisynthetic derivatives: Dihydroartemisinin (DHA), Artemether (AM) and Artesunate (AS). C) Schematic representation of stereochemical selectivity of the new multicomponent crystals (MCCs).

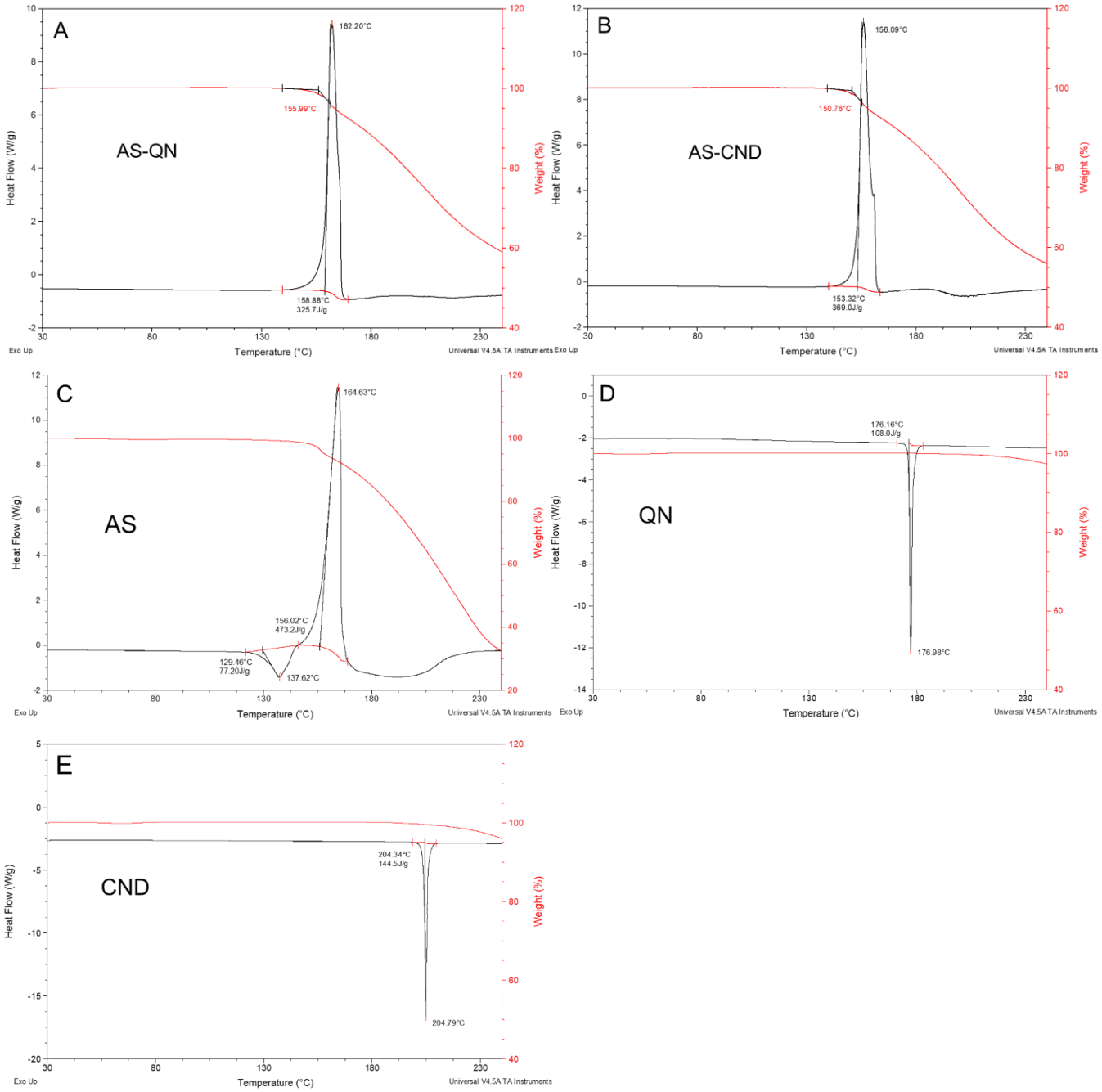

Figure S3. Differential scanning calorimetry (DSC) profiles of all the crystalline forms: A) AS-QN; B) AS-CND; C) AS; D) QN; E) CND. The scanning temperature range is 20 °C to 250 °C with heating ramp 10 °C/min. All heat flow values are based on exothermal upside.

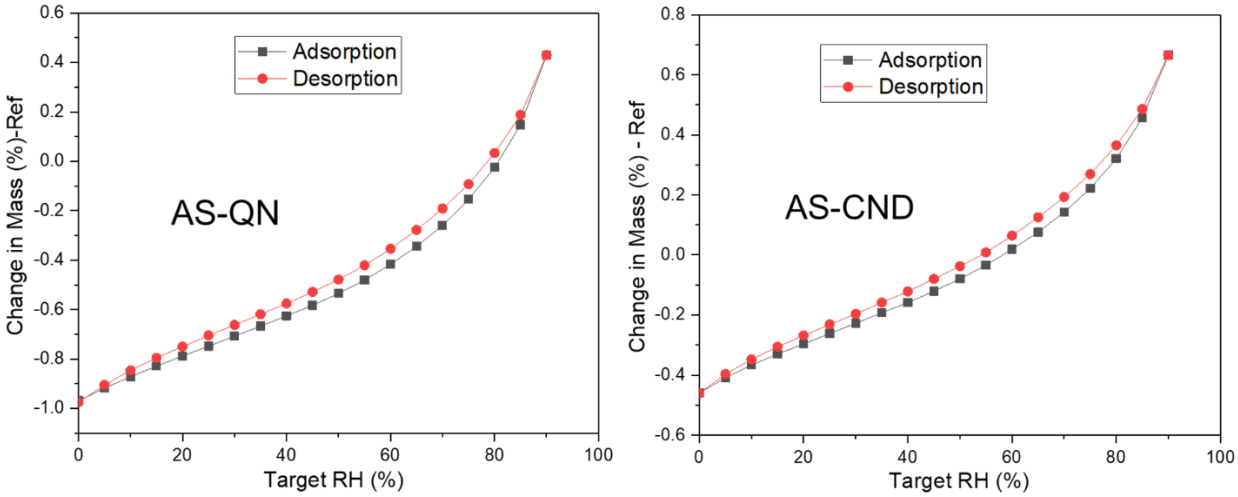

Figure S4. Dynamic Vapor Sorption (DVS) for AS-QN and AS-CND samples at 25 °C. The isotherm range is from 0 to 90 % RH and dm/dt = 0.002 for equilibrium at each humidity point.

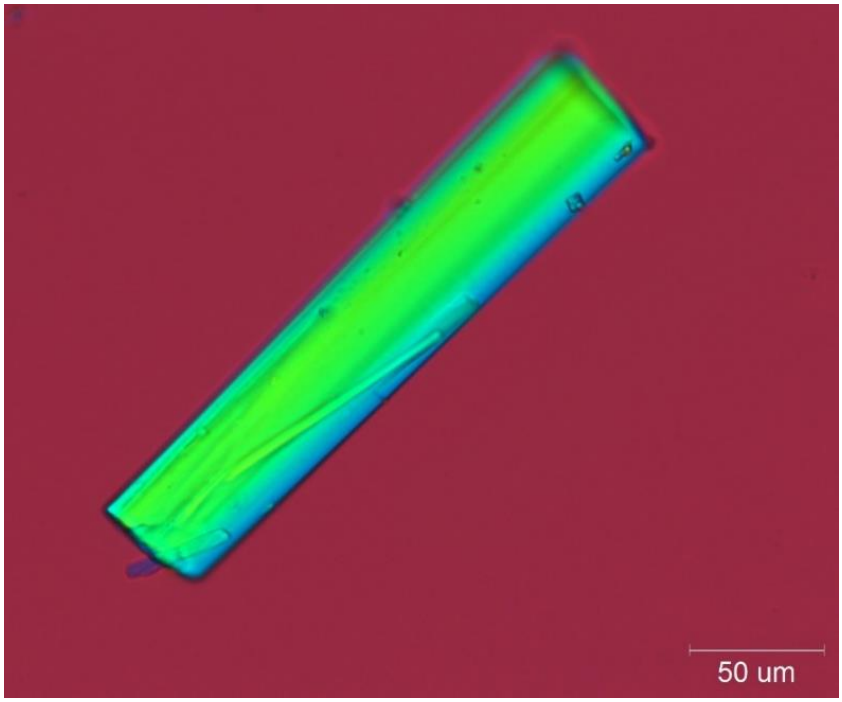

Figure S5. Polarized light microscope (PLM) image of the single crystal of AS-CND grown from slow solvent diffusion in isopropanol/n-heptane.

Table S1. Crystal Structure data and structural refinement information for AS-CND single crystal

Empirical formula	$C_{38}H_{50}N_2O_9$
Formula weight	678.80
Temperature/K	100
Crystal system	monoclinic
Space group	C2
a/Å	30.0476(16)
b/Å	6.6972(3)
c/Å	21.9220(12)
α/°	90
β/°	127.752(7)
γ/°	90
Volume/Å^3	3488.0(4)
Z	4
ρ_{calc}g/cm^3	1.293
μ/mm^{-1}	0.749
F(000)	1456.0
Radiation	CuKα (λ = 1.54178)
2Θ range for data collection/°	5.098 to 133.506
Index ranges	-35 ≤ h ≤ 35, -7 ≤ k ≤ 7, -26 ≤ l ≤ 26
Reflections collected	62257
Independent reflections	6129 [R_{int} = 0.1276, R_{sigma} = 0.0591]
Data/restraints/parameters	6129/1/454
Goodness-of-fit on F^2	1.077
Final R indexes [I>=2σ (I)]	R_1 = 0.0691, wR_2 = 0.1546
Final R indexes [all data]	R_1 = 0.0789, wR_2 = 0.1595
Largest diff. peak/hole / e Å^{-3}	0.35/-0.24
Flack parameter	-0.5(3)

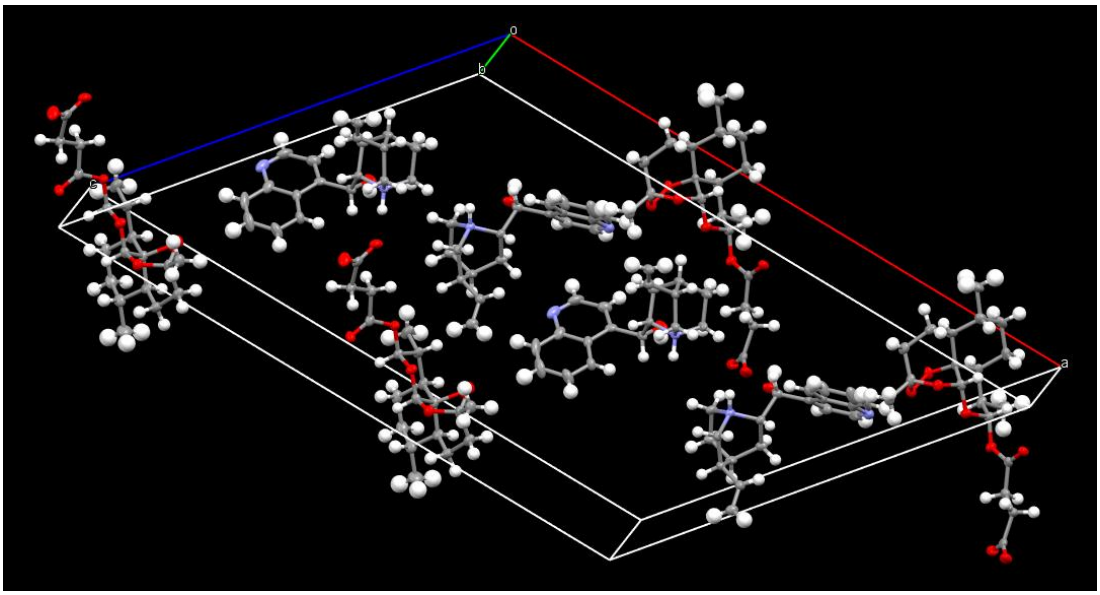

Figure S6. Crystal unit cell packing from AS-CND single crystal structures. The stoichiometry of AS: CND is 1:1 with 4 molecules each in one unit cell according to the monoclinic space group *C*2 with *Z*=4.

Table S2. CASTEP DFT Calculation Parameters

Parameter	Value
CASTEP calculation quality	Fine
Functional	GGA/PBE
DFT-D Correction	TS
Spin Polarization	Non-polarized
Geometry optimization method	LBFGS
Energy cutoff	600 eV
SCF tolerance	Fine (1.0e-6 eV/atom)
k-point separation	0.05 1/Å
Relativistic treatment	Koelling-Harmon

Table S3. ^{1}H-^{13}C CP-TOSS/MAS and CPPI/MAS (ν_{rot} = 12 kHz) experimental SSNMR parameters

Parameter	Value
Recycle delay (s)	1.69-19.5 (Optimized per sample using 1.3*T_1(^{1}H))
1H 90° pulse length (μs)	2.6
Contact time (ms)	4
^{1}H rf field during contact pulse (kHz)	96
^{13}C rf field during contact pulse & TOSS (kHz)	55.7
SPINAL-64 decoupling rf field (kHz)	96
Spectral width (kHz)	30242
Acquisition length (number of points)	4096
Steps in TOSS phase cycle	243
CPPI polarization inversion time (CPPI only) (μs)	50

Table S4. ^{1}H-^{13}C FSLG-HETCOR (ν_{rot} = 12 kHz) additional experimental SSNMR parameters[a]

Parameter	Value
Contact pulse (ms)	0.1
+LG frequency offset	66245.7
−LG frequency offset	-70245.7
^{1}H evolution offset (Hz)	-2000
LG RF field (kHz)	96.5
Number of scans	8
Indirect dimension acquisition length (number of points)	128
2D Acquisition mode	STATES-TPPI

[a] Other relevant parameters are identical to those in the CP-TOSS experiments.

Table S5. Comparison of experimental and calculated ^{13}C SSNMR chemical shifts. Atom numbering for the starting materials are shown below the tables. For the MCCs, atom numbering is consistent with those in the included crystal structures.

AS Atom	Calc ^{13}C Shift	Expt. ^{13}C Shift	Difference	CND Atom	Calc ^{13}C Shift	Expt. ^{13}C Shift	Difference
C_16	176.6	171.83	4.77	C_11	151.7	150.62	-1.08
C_19	175.5	171.83	3.67	C_13	153.2	149.51	-3.69
C_5	111.2	105.48	5.72	C_19	148.4	148.5	0.1
C_12	96.8	92.99	3.81	C_9	149.2	143.51	-5.69
C_6	96.1	91.62	4.48	C_18	131.5	130.46	-1.04
C_1	83.5	79.97	3.53	C_17	129.2	128.49	-0.71
C_2	51.5	51.41	0.09	C_16	126.6	126.34	-0.26
C_7	44.3	43.92	0.38	C_14	125.8	125.89	0.09
C_10	36.8	37.31	-0.51	C_15	122.6	122.09	-0.51
C_4	33.4	35.9	-2.5	C_12	118.6	118.66	0.06
C_9	31.1	34.03	-2.93	C_10	111.2	110.73	-0.47
C_13	28.8	30.54	-1.74	C_8	70.4	69.68	-0.72
C_17	26.3	28.41	-2.11	C_7	**61.7**	61.32	-0.38
C_18	24.9	27.81	-2.91	C_1	58.5	59.51	1.01
C_3	20.7	23.68	-2.98	C_5	42.6	44.74	2.14
C_15	19.8	24.16	-4.36	C_2	41.3	41.65	0.35
C_8	18.7	20.98	-2.28	C_3	26.3	28.24	1.94
C_11	16.2	19.73	-3.53	C_4	22.9	26.48	3.58
C_14	7.1	10.46	-3.36	C_6	17.1	20.39	3.29
		RMSD:	3.276887			RMSD:	2.091382

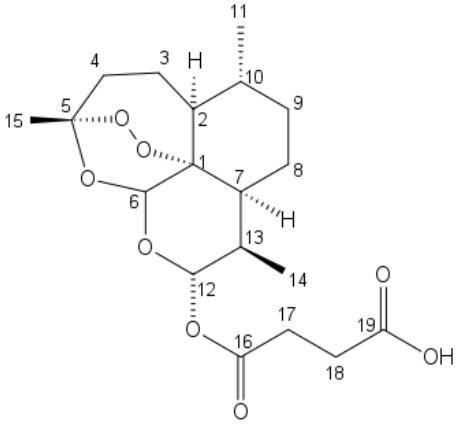

AS Numbering

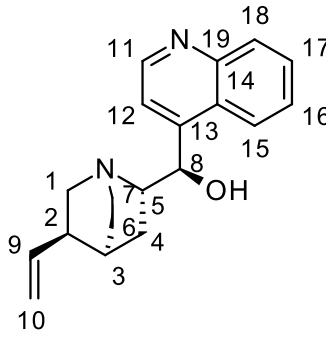

CND Numbering

QN			
Atom	Calc ^{13}C Shift	Expt. ^{13}C Shift	Difference
C_56	160.2	158.29	-1.91
C_36	160	157.84	-2.16
C_16	158.7	157.03	-1.67
C_53	157	153.01	-3.99
C_33	156.6	152.48	-4.12
C_13	156.2	151.78	-4.42
C_9	150.1	146.44	-3.66
C_29	149.3	146.02	-3.28
C_49	146.5	145.87	-0.63
C_11	146.3	145.87	-0.43
C_51	145	142.73	-2.27
C_31	144.5	142.73	-1.77
C_59	142.7	143.81	1.11
C_19	142.6	143.58	0.98
C_39	142.4	142.53	0.13
C_58	131.9	131.28	-0.62
C_38	131.7	131.13	-0.57
C_18	131.5	130.93	-0.57
C_54	127.1	126.71	-0.39
C_34	126.6	126.3	-0.3
C_14	126.4	126.03	-0.37
C_57	125.1	124.36	-0.74
C_37	123.3	124.21	0.91
C_17	122.2	122.73	0.53
C_52	117.8	117.37	-0.43
C_32	117.3	117.06	-0.24
C_12	116.5	116.9	0.4
C_50	116.5	113.87	-2.63
C_10	116.3	113.44	-2.86
C_30	113.9	113.22	-0.68
C_55	100.7	100.6	-0.1
C_15	100.2	99.3	-0.9
C_35	99	98.9	-0.1
C_48	72.8	70.9	-1.9
C_8	72.5	70.75	-1.75
C_28	71.8	70.18	-1.62
C_47	63.7	61.85	-1.85
C_27	62.5	61.37	-1.13
C_7	61.2	59.34	-1.86
C_25	59.5	58.76	-0.74
C_45	59	58.38	-0.62
C_5	58	57.71	-0.29
C_60	54.4	54.98	0.58
C_40	51.4	52.17	0.77
C_20	50.8	52.17	1.37
C_21	45.5	44.89	-0.61
C_41	44.1	44.54	0.44
C_1	42.7	43.7	1
C_44	42.3	42.59	0.29
C_4	42.1	41.63	-0.47
C_24	41.4	40.56	-0.84
C_43	29.8	30.77	0.97
C_3	29.4	29.56	0.16
C_2	27.3	29.36	2.06
C_23	26.9	28.54	1.64
C_42	26.7	28.82	2.12
C_22	25.8	28.82	3.02
C_6	17	19.27	2.27
C_46	16.5	19.12	2.62
C_26	16.3	18.83	2.53
		RMSD:	1.743621

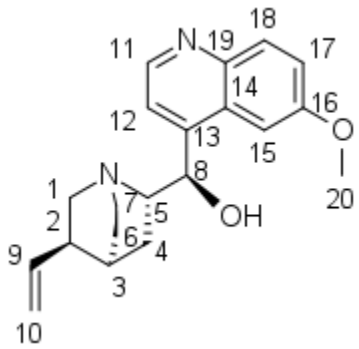

QN Numbering

(Numbering for second and third molecules follows the same order, starting at 21, and 41, respectively)

QN HCl•2H$_2$O				AS-CND (Salt)				AS-CND (Cocrystal)			
Atom	Calc.	Expt.	Diff.	Atom	Calc.	Expt.	Diff.	Atom	Calc.	Expt.	Diff.
C_21	159.8581	158.61	-1.24809	C_19	176.9	176.7	-0.2	C_19	184.8	176.7	-8.14982
C_23	159.7019	158.61	-1.09191	C_16	176.5	172.39	-4.11	C_16	175.8	172.39	-3.40564
C_10	146.2054	146.49	0.284578	C_26	151.7	149.81	-1.89	C_26	152.2	149.81	-2.41084
C_7	145.3562	146.49	1.133773	C_28	149.6	147.35	-2.25	C_28	150.6	147.35	-3.26626
C_1	144.6807	143.99	-0.69066	C_25	147.1	145.83	-1.27	C_25	147.2	145.83	-1.32048
C_30	144.3417	139.62	-4.72173	C_37	140.7	136.86	-3.84	C_37	143.4	136.86	-6.55966
C_35	144.0648	139.62	-4.44477	C_20	133.5	131.82	-1.68	C_20	134.7	131.82	-2.87944
C_4	143.8552	142.94	-0.9152	C_21	130.4	129.18	-1.22	C_21	129.7	129.18	-0.49443
C_2	143.1516	142.94	-0.21161	C_22	128.9	127.92	-0.98	C_22	127.5	127.92	0.391977
C_15	143.065	142.94	-0.12498	C_38	127.6	123.7	-3.9	C_38	124.7	123.7	-0.96442
C_12	132.4775	131.07	-1.40753	C_24	124.1	124.18	0.08	C_24	124.1	124.18	0.102018
C_6	131.2064	131.07	-0.13645	C_23	122.4	122.09	-0.31	C_23	121.1	122.09	1.009649
C_9	126.5316	125.81	-0.72158	C_27	118.5	118.3	-0.2	C_27	118.4	118.3	-0.09493
C_29	125.9684	125.81	-0.15837	C_10	107.6	103.08	-4.52	C_10	107.6	103.08	-4.54257
C_40	123.8265	122.23	-1.59654	C_12	95.1	91.41	-3.69	C_12	95.1	91.41	-3.70106
C_20	122.2133	118.82	-3.39328	C_13	94.4	91.41	-2.99	C_13	94.7	91.41	-3.29297
C_31	121.9795	118.82	-3.15952	C_6	83	80.07	-2.93	C_6	82.7	80.07	-2.66058
C_8	118.3381	118.82	0.481869	C_29	69.4	67.68	-1.72	C_29	73.8	67.68	-6.13752
C_39	118.2754	117.39	-0.88544	C_30	61.4	60.64	-0.76	C_30	64.0	60.64	-3.37819
C_3	116.2163	118.82	2.603695	C_35	53.7	55.56	1.86	C_35	57.0	55.56	-1.4869
C_18	100.725	99.51	-1.21496	C_7	51.5	52.59	1.09	C_7	51.4	52.59	1.198456
C_22	99.8216	99.51	-0.3116	C_34	41.9	44.12	2.22	C_34	43.8	44.12	0.312758
C_19	70.17725	65.83	-4.34725	C_5	41.6	42.74	1.14	C_5	41.5	42.74	1.280568
C_13	67.34267	65.83	-1.51267	C_36	37.9	39.75	1.85	C_36	40.1	39.75	-0.38578
C_28	61.28205	61.77	0.487955	C_2	34.3	36.75	2.45	C_2	34.5	36.75	2.209826
C_17	59.76549	61.77	2.004511	C_9	34.2	36.25	2.05	C_9	34.2	36.25	2.052052
C_37	55.28653	56.44	1.153467	C_3	32.7	35.07	2.37	C_18	33.6	35.07	1.448715
C_27	55.16111	57.07	1.908887	C_18	32.2	33.91	1.71	C_3	33.1	33.91	0.80881
C_32	54.66369	57.07	2.40631	C_14	30.2	32.25	2.05	C_14	29.8	32.25	2.475397
C_38	53.81451	56.44	2.625492	C_17	28.2	31.23	3.03	C_17	25.7	31.23	5.534629
C_11	44.49134	44.72	0.228658	C_32	25.2	27.93	2.73	C_32	25.7	27.93	2.242722
C_5	43.34321	43.75	0.406794	C_11	23.1	27.43	4.33	C_33	24.6	27.43	2.872887
C_26	37.16591	38.32	1.154091	C_33	22.5	26.14	3.64	C_11	23.0	26.14	3.147257
C_16	37.08226	38.32	1.237736	C_8	21	24.23	3.23	C_8	21.1	24.23	3.089636
C_36	23.45882	27.95	4.49118	C_4	19.8	22.38	2.58	C_4	19.8	22.38	2.58643
C_24	22.58047	27.95	5.369534	C_1	16.3	19.87	3.57	C_1	16.6	19.87	3.316479
C_25	22.01362	25.06	3.04638	C_31	14.2	18.13	3.93	C_31	14.7	18.13	3.445749
C_33	20.10277	23.6	3.497233	C_15	5.8	10.89	5.09	C_15	5.7	10.89	5.190459
C_14	16.38854	19.19	2.801459								
C_34	15.03947	19.19	4.150525	AS				AS			
		RMSD:	2.373149	CND		RMSD:	2.688781	CND		RMSD:	3.222632

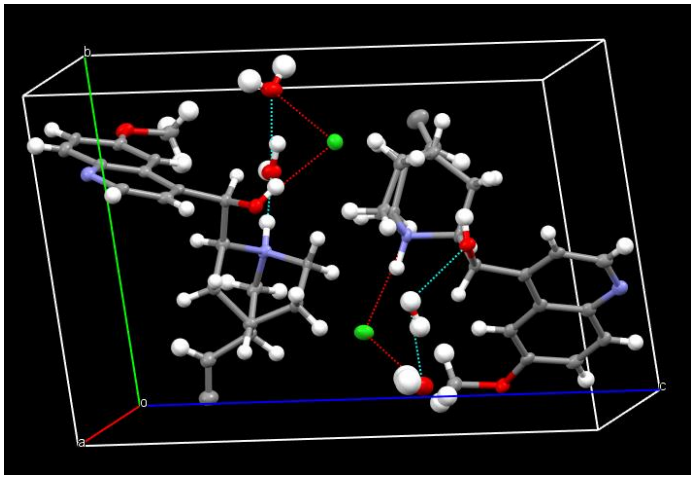

Figure S7. Crystal unit cell packing from Quinine hydrochloride dihydrate (QN HCl·2H_2O) single crystal structures. The stoichiometry of QN:HCl:H_2O is 1:1:2 according to the triclinic space group *P*1 with *Z*=2. From the single crystal structure, it is clearly to see the aliphatic amine group in QN molecule is protonated.

Table S6. Crystal Structure data and structural refinement information for QN HCl·2H_2O single crystal

Empirical formula	$C_{20}H_{29}ClN_2O_4$
Formula weight	396.90
Temperature/K	100
Crystal system	triclinic
Space group	P1
a/Å	6.7848(3)
b/Å	10.6171(5)
c/Å	15.4805(8)
α/°	98.689(2)
β/°	97.586(2)
γ/°	108.323(2)
Volume/Å^3	1027.12(9)
Z	2
ρ_{calc}g/cm^3	1.283
μ/mm^{-1}	1.873
F(000)	424.0
Radiation	CuKα (λ = 1.54178)
2Θ range for data collection/°	5.884 to 134.49
Index ranges	-8 ≤ h ≤ 8, -12 ≤ k ≤ 12, -18 ≤ l ≤ 18
Reflections collected	28580
Independent reflections	6948 [R_{int} = 0.0553, R_{sigma} = 0.0435]
Data/restraints/parameters	6948/3/533
Goodness-of-fit on F^2	1.099
Final R indexes [I>=2σ (I)]	R_1 = 0.0804, wR_2 = 0.2147
Final R indexes [all data]	R_1 = 0.0816, wR_2 = 0.2213
Largest diff. peak/hole / e Å^{-3}	0.61/-0.41
Flack parameter	0.05(2)

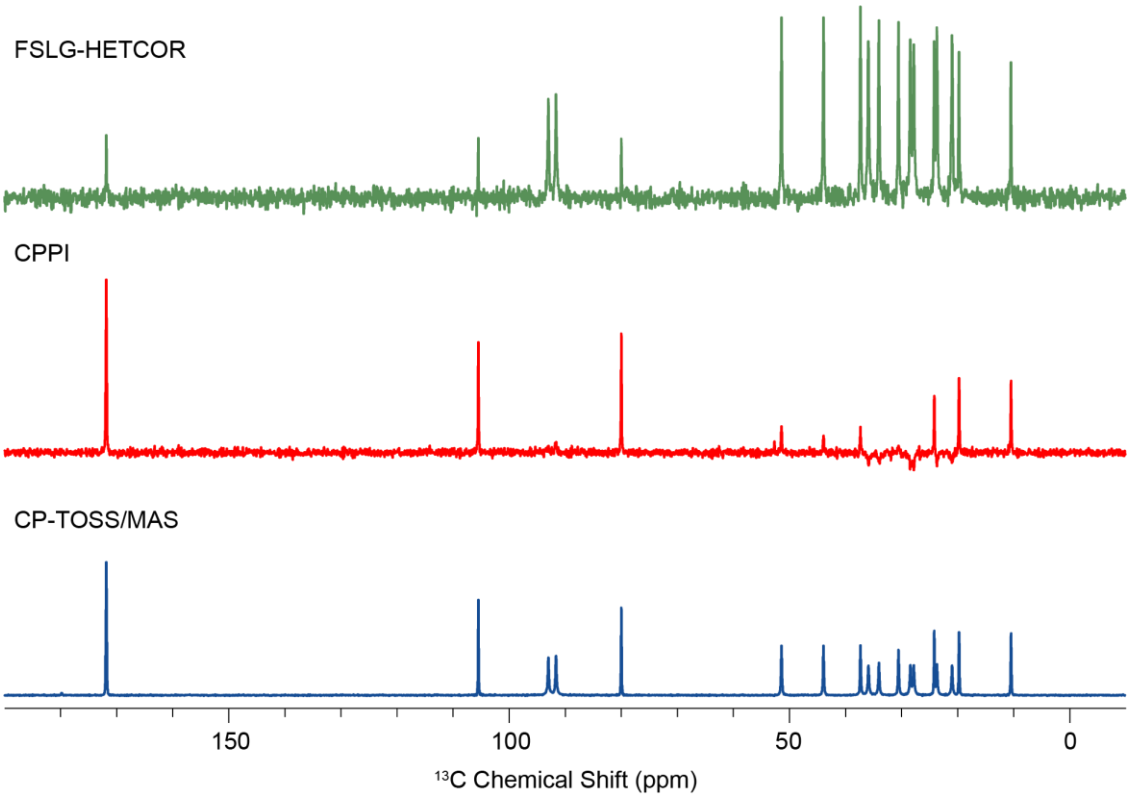

Figure S8. ^{13}C MAS (ν_{rot} = 12 kHz) SSNMR spectra used for peak assignments of AS. Bottom: CP-TOSS spectrum, middle: CPPI spectrum (CH_3 & C positive phase, CH null, CH2 negative phase), top: projection of the 2D FSLG-HETCOR spectrum.

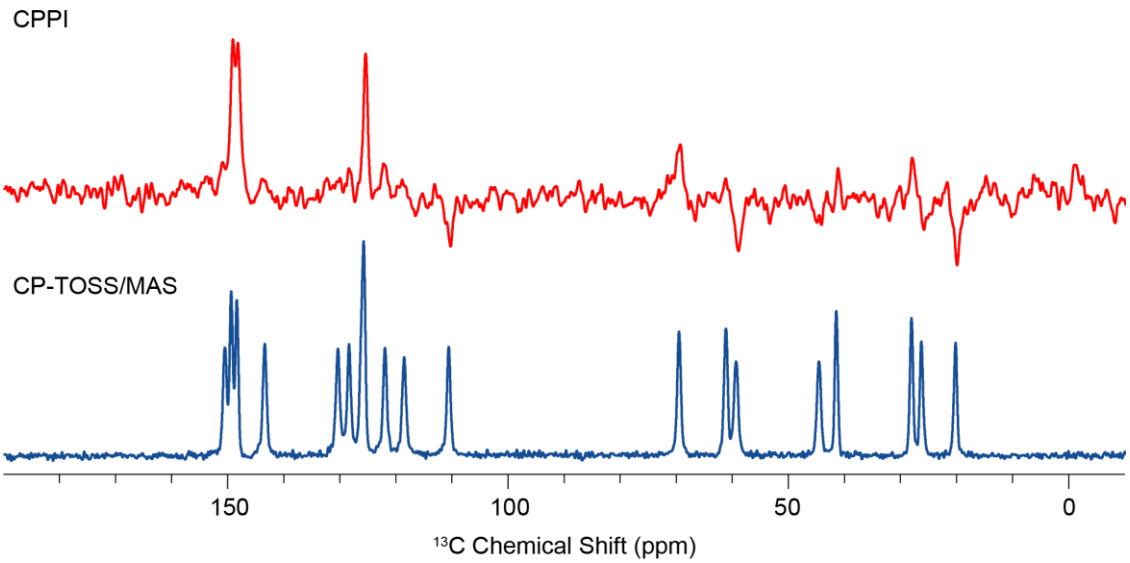

Figure S9. ^{13}C MAS (ν_{rot} = 12 kHz) SSNMR spectra used for peak assignments of CND. Bottom: CP-TOSS spectrum, top: CPPI spectrum (CH_3 & C positive phase, CH null, CH2 negative phase). FSLG-HETCOR spectrum not acquired due to long $T_1(^1H)$.

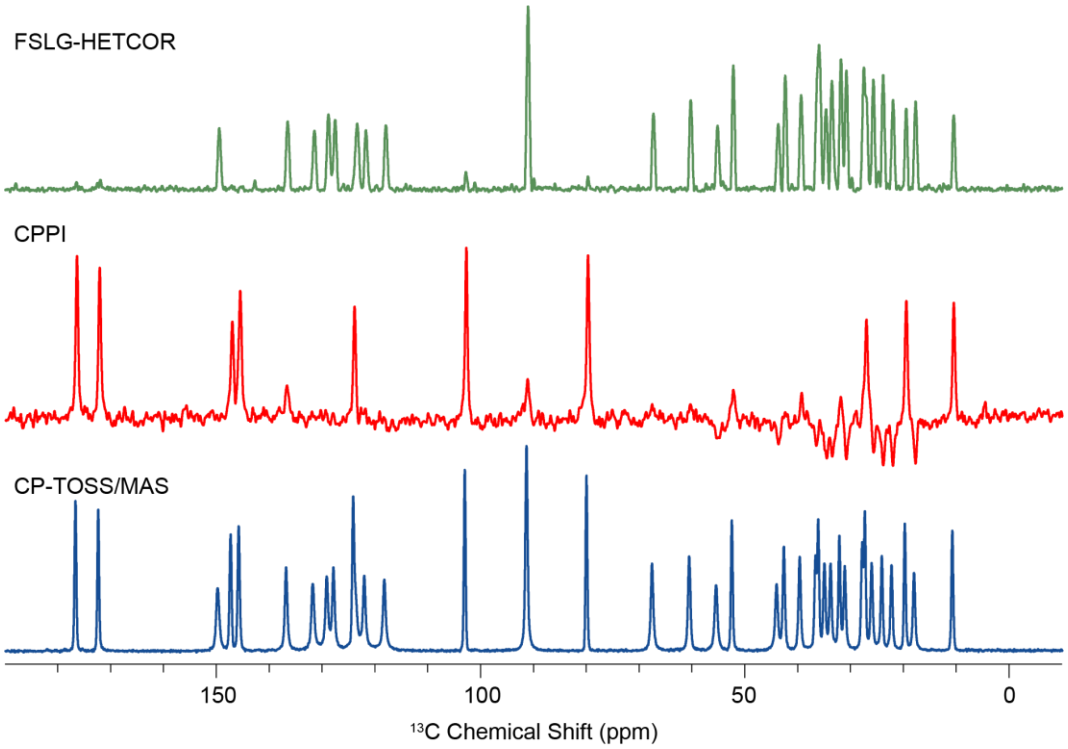

Figure S10. ^{13}C MAS (ν_{rot} = 12 kHz) SSNMR spectra used for peak assignments of AS-CND. Bottom: CP-TOSS spectrum, middle: CPPI spectrum (CH_3 & C positive phase, CH null, CH2 negative phase), top: projection of the 2D FSLG-HETCOR spectrum.

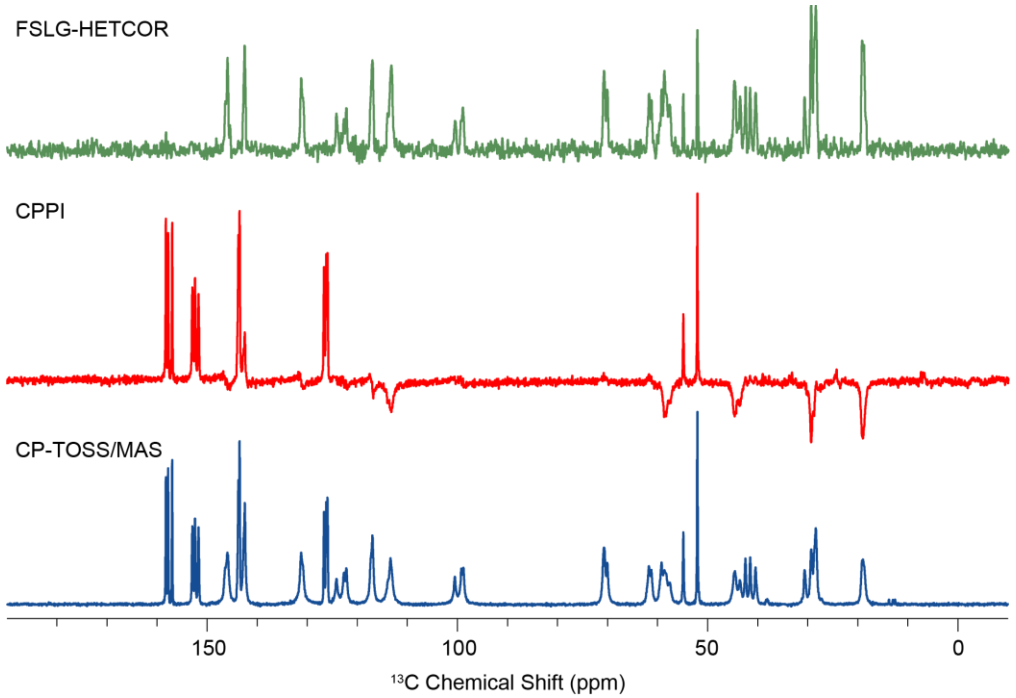

Figure S11. ^{13}C MAS (ν_{rot} = 12 kHz) SSNMR spectra used for peak assignments of QN. Bottom: CP-TOSS spectrum, middle: CPPI spectrum (CH_3 & C positive phase, CH null, CH2 negative phase), top: projection of the 2D FSLG-HETCOR spectrum.

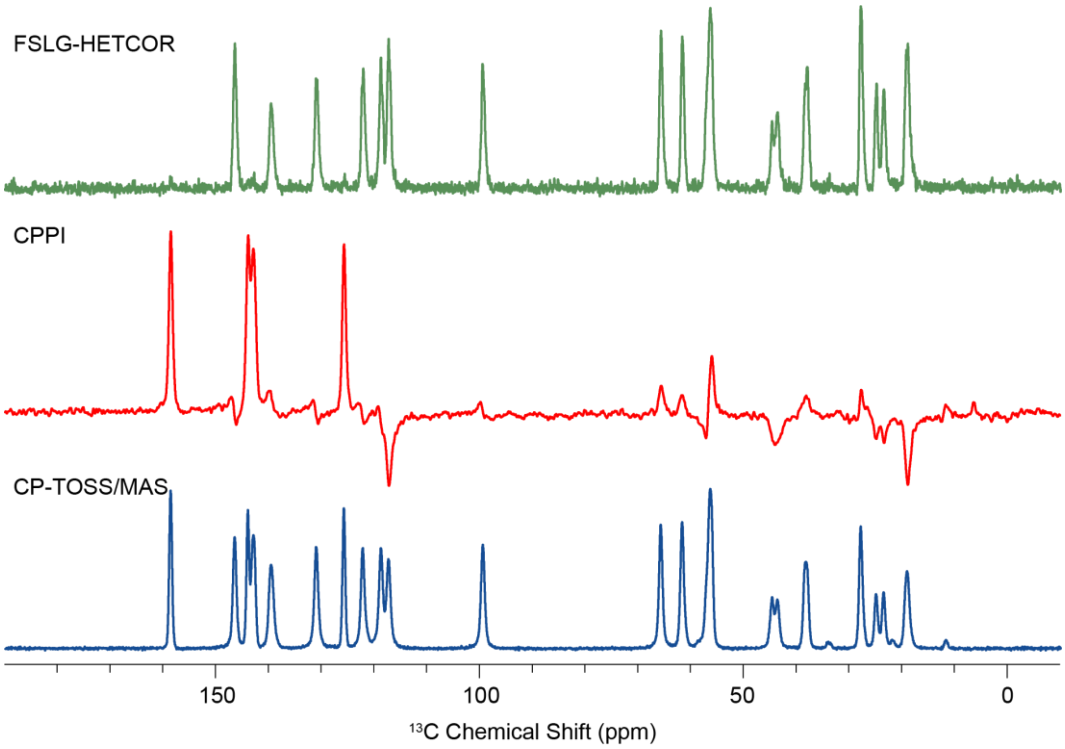

Figure S12. ^{13}C MAS (ν_{rot} = 12 kHz) SSNMR spectra used for peak assignments of QN HCl•2H_2O. Bottom: CP-TOSS spectrum, middle: CPPI spectrum (CH_3 & C positive phase, CH null, CH2 negative phase), top: projection of the 2D FSLG-HETCOR spectrum.

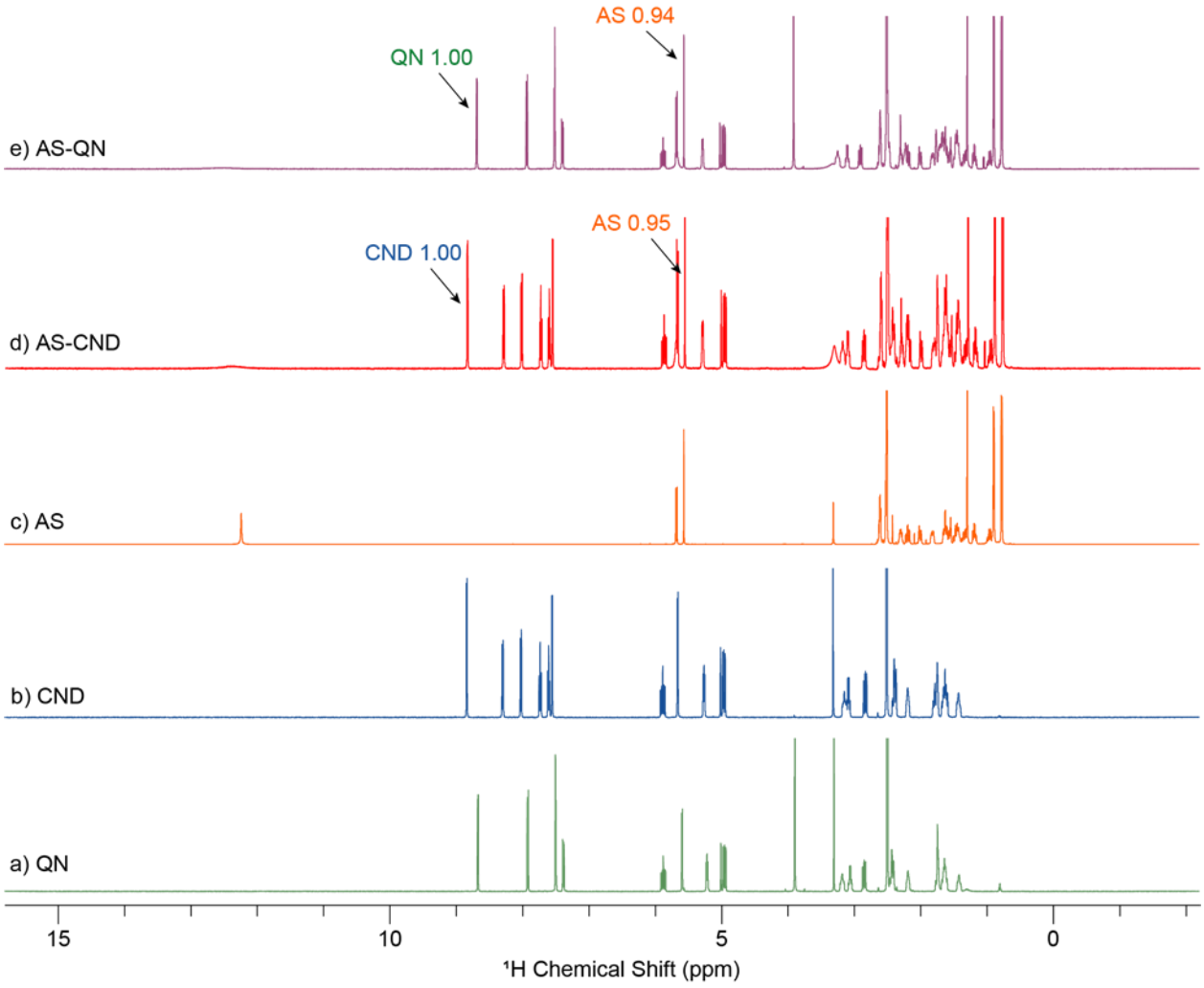

Figure S13. ^{1}H Solution NMR spectra of the starting materials and MCCs: a) QN; b) CND; c) AS; d) AS-CND; e) AS-QN. Peaks used for determination of the MCC stoichiometry are highlighted with arrows and their corresponding integrated values.

Table S7. ^{1}H experimental solution NMR parameters

Parameter	Value
Solvent	DMSO-d_6; 99.9% (Sigma Aldrich)
Concentration (mg/mL)	*ca*. 50
Temperature (K)	300
Sweep width (Hz)	12376
Excitation pulse angle	10°
Recycle delay (s)	2
Number of scans	128

Table S8. ^{1}H-^{15}N CP/MAS (ν_{rot} = 12 kHz) experimental SSNMR parameters

Parameter	Value
Recycle delay (s)	1.69-19.5 (Optimized per sample using 1.3*T_1(^{1}H))
1H 90° pulse length (µs)	2.6
Contact time (ms)	3
^{1}H rf field during contact pulse (kHz)	60
^{15}N rf field during contact pulse & TOSS (kHz)	25
SPINAL-64 decoupling rf field (kHz)	96
Spectral width (kHz)	30242
Acquisition length (number of points)	4096

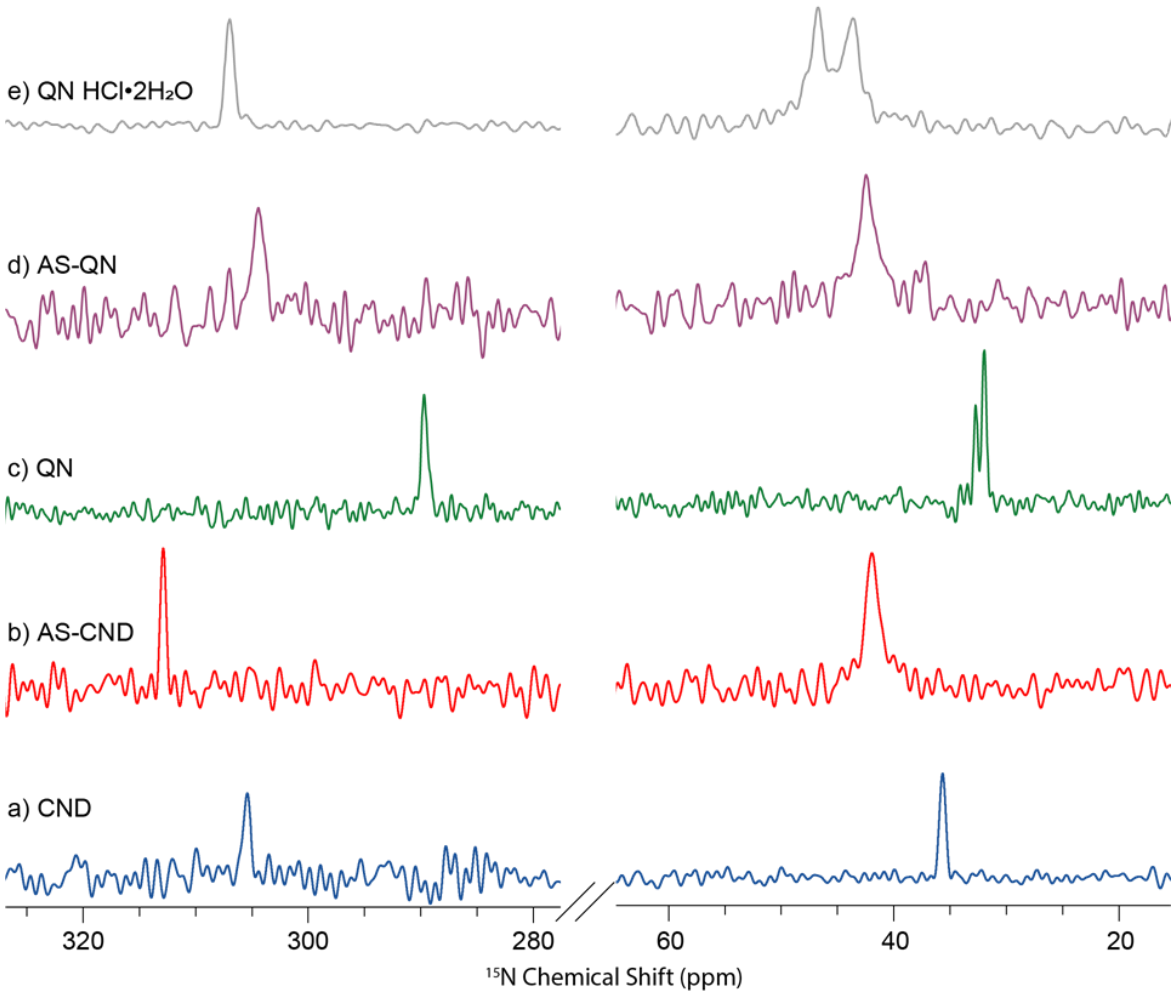

Figure S14. ^{1}H-^{15}N CP/MAS (ν_{rot} = 12 kHz) SSNMR spectra showing expanded regions around the peaks.

Table S9. Experimental and calculated isotropic ^{15}N chemical shifts for the nitrogen-containing compounds in this work.

	R_2N Shift (ppm)		R_3N(-H?) Shift (ppm)		
Compound	**Expt.**	**Calc.**	**Expt.**	**Calc.**	**RMSE (ppm)**
CND	305.4	305.3	35.6	34.3	0.9
AS-CND Salt	312.8	313	41.9	41.7	0.2
AS-CND Cocrystal[a]		310.4		29.2	9.1
QN	290	282.45 281.62 279.63	32.9 32.2 32.0	29.52 29.10 29.10	6.6
AS-QN	304.6	–	42.7	–	–
QN HCl·2H_2O	306.8	305.81 301.36	46.8 43.9	47.57 46.32	3.9

[a] Structure generated from the AS-CND salt structure by replacing the hydrogen bound to the aliphatic amine with one bound to the carboxylic acid (r_{O-H} = 1.10 Å, r_{N-H} = 1.72 Å)

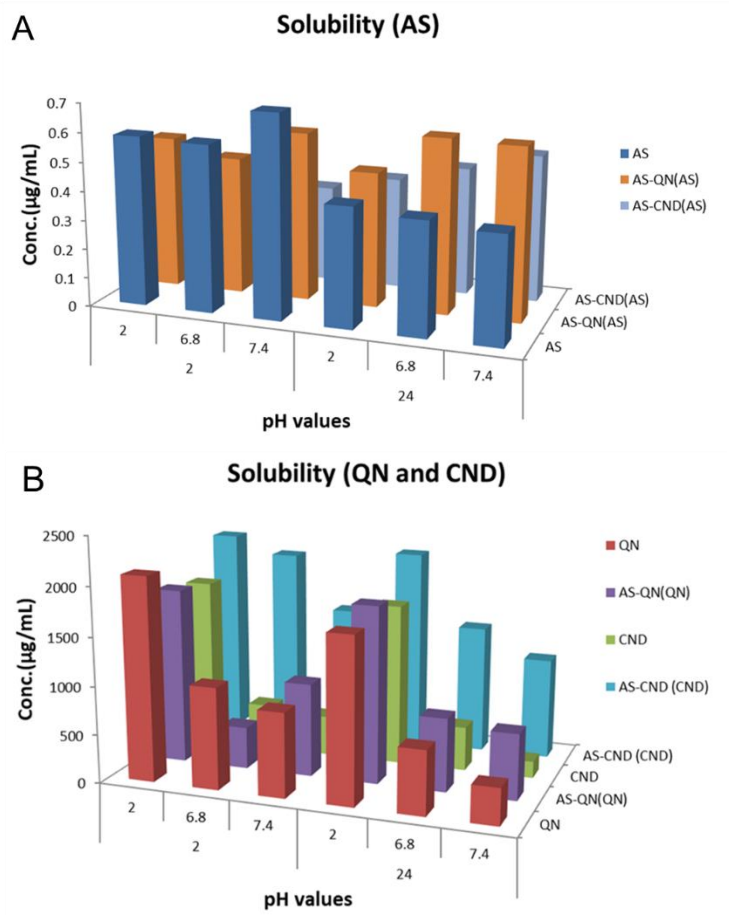

Figure S15. Experimental solubility results for both MCCs and all starting materials (AS, QN and CND) in PBS buffer solution at room temperature with three different pH values: 2.0, 6.8 and 7.4. for 2h and 24 h. A) Solubility of AS and B) Solubility of QN and CND.

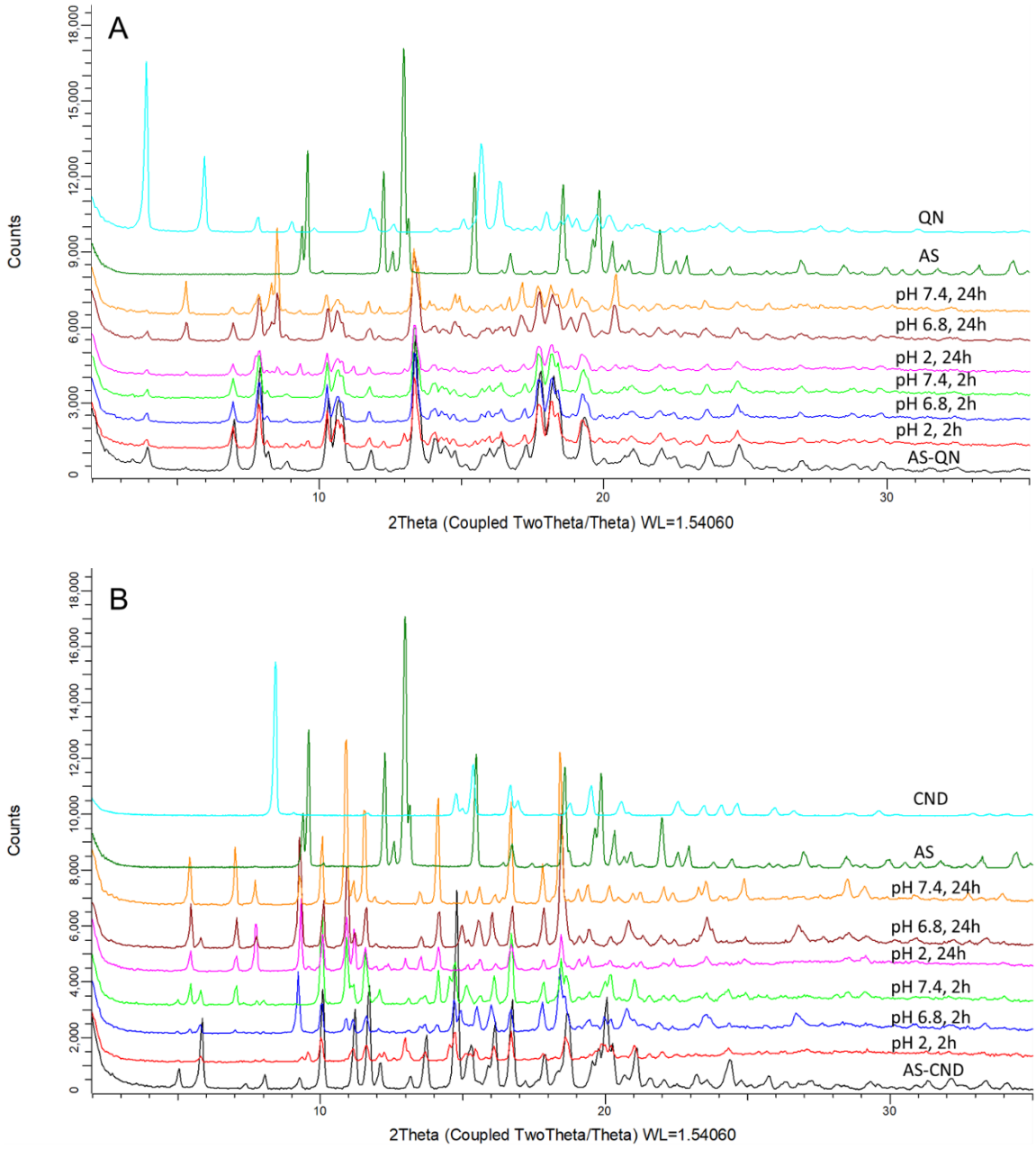

Figure S16. PXRD patterns MCCs after solubility test (PBS buffer solution at 25 C)in different conditions. All PXRD patterns are compared with the starting materials and corresponding single components. A) AS-QN and B) AS-CND.

Table S10. Solubility data of both salts and single components in PBS buffer solution with three different pH values for 2 hr and 24 hr equilibrium time.

Time (hr)	pH	Solubility of Single Components (μg/mL)			Solubility of Salts (μg/mL)			
		AS	QN	CND	AS-QN salt		AS-CND salt	
					AS	QN	AS	CND
2	2.0	0.5845	2097.5	1748.2	0.5279	1811.1	0.3675	2148.6
	6.8	0.5751	1046.7	467.57	0.4746	432.02	0.4200	1975.3
	7.4	0.697	869.74	411.59	0.5817	959.31	0.3352	1404.5
24	2.0	0.4123	1694.7	1661.5	0.4651	1815.4	0.3867	2069.9
	6.8	0.3903	658.13	453.03	0.6007	754.28	0.4451	1324.8
	7.4	0.3708	375.82	171.33	0.5925	676.13	0.5087	1043.9

Reference

[1] D. Hasa, W. Jones, *Adv. Drug Deliv. Rev.* **2017**, 117, 147-161.

[2] DIFFRAC EVA (version 5.2.0.3), program for powder X-ray diffraction, Bruker AXS, Madison, WI, **2020**.

[3] APEX 3 (version 2018.7-2), program for Bruker X8 diffractometer control, Bruker AXS, Madison, WI, **2018**.

[4] OLEX 2 (version 1.3.0) a) O. V.Dolomanov, L. J. Bourhis, R. J. Gildea, J. A. K. Howard, H. Puschmann, *J. Appl. Cryst.* **2009**, 42, 339-341. b) G. M. Sheldrick, *Acta Cryst. A* **2015**, 71, 3-8. c) G. M. Sheldrick, *Acta Cryst. A* **2008**, 64, 112-122.

[5] R. K. Harris, E. D. Becker, S. M. C. de Menezes, R. Goodfellow, P. Granger, *Pure Appl. Chem.* **2001**, *73*, 1795–1818.

[6] P. Bertani, J. Raya, B. Bechinger, *Solid State Nucl. Mag.* **2014**, *61*, 15–18.

[7] O. B. Peersen, X. L. Wu, S. O. Smith, *J. Magnetic Reason. Ser.* **1994**, *106*, 127–131.

[8] O. B. Peersen, X. L. Wu, I. Kustanovich, S. O. Smith, *J. Magnetic Reason. Ser.* **1993**, *104*, 334–339.

[9] G. Metz, X. L. Wu, S. O. Smith, *J. Magnetic Reason. Ser.* **1994**, *110*, 219–227.

[10] B. M. Fung, A. K. Khitrin, K. Ermolaev, *J. Magn. Reason.* **2000**, *142*, 97–101.

[11] Z. Song, O. N. Antzutkin, X. Feng, M. H. Levitt, *Solid State Nucl. Mag.* **1993**, *2*, 143–146.

[12] X. L. Wu, K. W. Zilm, *J. Magnetic Reson. Ser.* **1993**, *102*, 205–213.

[13] B.-J. van Rossum, H. Förster, H. J. M. de Groot, *J Magn. Reson.* **1997**, *124*, 516–519.

[14] M. C. Payne, M. P. Teter, D. C. Allan, T. A. Arias, J. D. Joannopoulos, *Rev. Mod. Phys.* **1992**, *64*, 1045–1097.

[15] C. Bonhomme, C. Gervais, F. Babonneau, C. Coelho, F. Pourpoint, T. Azaïs, S. E. Ashbrook, J. M. Griffin, J. R. Yates, F. Mauri, C. J. Pickard, *Chem. Rev.* **2012**, *112*, 5733–5779.

[16] C. J. Pickard, F. Mauri, *Phys. Rev. B* **2001**, *63*, 245101.

[17] J. P. Perdew, K. Burke, M. Ernzerhof, *Phys. Rev. Lett.* **1996**, *77*, 3865–3868.

[18] A. Tkatchenko, M. Scheffler, *Phys. Rev. Lett.* **2008**, *102*, 073005.

[19] J. J. Walsh, D. Coughlan, N. Heneghan, C. Gaynor, A. Bell, *Bioorg. Med. Chem. Lett.* **2007**, 17, 3599–3602.

[20] A. Çapcı, M. M. Lorion, H. Wang, N. Simon, M. Leidenberger, M. C. Borges Silva, D. R. M. Moreira, Y. Zhu, Y. Meng, J. Y. Chen, Y. M. Lee, O. Friedrich, B. Kappes, J. Wang, L. Ackermann, S. B. Tsogoeva, *Angew. Chem. Int. Ed.* **2019**, *58*, 13066-13079.